Journal of Quantitative Spectroscopy & Radiative Transfer 147 (2014) 171–177

Contents lists available at ScienceDirect

Journal of Quantitative Spectroscopy & Radiative Transfer

journal homepage: www.elsevier.com/locate/jqsrt

Rayleigh scattering cross-section measurements of nitrogen, argon, oxygen and air

Ryan Thalman [a,b,1], Kyle J. Zarzana [a,b], Margaret A. Tolbert [a,b], Rainer Volkamer [a,b,*]

[a] Department of Chemistry and Biochemistry, University of Colorado, Boulder, CO, USA
[b] Cooperative Institute for Research in Environmental Sciences (CIRES), Boulder, CO, USA

ARTICLE INFO

Article history:
Received 7 March 2014
Received in revised form
28 May 2014
Accepted 30 May 2014
Available online 9 June 2014

Keywords:
Rayleigh scattering
Refractive index theory
Ultraviolet
Visible spectral range
Cavity ring down spectroscopy
Broadband cavity enhanced spectroscopy

ABSTRACT

Knowledge about Rayleigh scattering cross sections is relevant to predictions about radiative transfer in the atmosphere, and needed to calibrate the reflectivity of mirrors that are used in high-finesse optical cavities to measure atmospheric trace gases and aerosols. In this work we have measured the absolute Rayleigh scattering cross-section of nitrogen at 405.8 and 532.2 nm using cavity ring-down spectroscopy (CRDS). Further, multi-spectral measurements of the scattering cross-sections of argon, oxygen and air are presented relative to that of nitrogen from 350 to 660 nm using Broadband Cavity Enhanced Spectroscopy (BBCES). The reported measurements agree with refractive index based theory within $0.2 \pm 0.4\%$, and have an absolute accuracy of better than 1.3%. Our measurements expand the spectral range over which Rayleigh scattering cross section measurements of argon, oxygen and air are available at near-ultraviolet wavelengths. The expressions used to represent the Rayleigh scattering cross-section in the literature are evaluated to assess how uncertainties affect quantities measured by cavity enhanced absorption spectroscopic (CEAS) techniques. We conclude that Rayleigh scattering cross sections calculated from theory provide accurate data within very low error bounds, and are suited well to calibrate CEAS measurements of atmospheric trace gases and aerosols.

1. Introduction

The theory and measurements of the scattering of light by gases has been studied for well over a century [1] and is vital to our understanding of radiative transfer in the Earth and other planetary atmospheres. The interaction of light (electromagnetic fields) with a wavelength much larger than the size of a molecule gives rise to the scattering of light. This effect known as Rayleigh scattering, accounts for scattering, local field effects (Lorentz–Lorenz) [2] as well as depolarization from the non-sphericity of particles (King correction factor) [3,4].

The cross-section, σ, for Rayleigh scattering can be calculated based on the refractive index of the gas as follows [5]:

$$\sigma(\nu) = \frac{24\pi^3\nu^4}{N^2}\left(\frac{n_\nu^2-1}{n_\nu^2+2}\right)^2 F_k(\nu), \quad (1)$$

where ν is the wavenumber of light (cm^{-1}), N is the number density of the gas, n_ν is the wavenumber dependent real refractive index and F_k is the King correction factor which accounts for the depolarization. Detailed derivation and explanation of the different influences on the scattering can be found elsewhere in the literature [5–9].

* Correspondence to: 215 UCB, Boulder, CO 80309, USA.
Tel.: +1 303 492 1843.
E-mail address: rainer.volkamer@colorado.edu (R. Volkamer).
[1] Now at: Brookhaven National Laboratory, 815-E, Upton, NY, USA.

http://dx.doi.org/10.1016/j.jqsrt.2014.05.030
0022-4073/

While measurements of the different components of scattering (correction factors, refractive index) have been performed for the better part of a century [2,10–13], there are surprisingly few laboratory measurements of Rayleigh scattering cross-sections [5,9,14–16]. In particular there is little data in the near-UV (300–420 nm) and what is available has large uncertainty.

Rayleigh scattering cross-section measurements in the literature have been carried out in two ways: (1) nephelometry [16]; and (2) cavity-ring down spectroscopy (CRDS) [5,9,14,15]. The pioneering nephelometry measurements of Shardanand and Rao [16] are the only work of its kind and consist of the direct measurement of scattered light at discrete angles and then the integration of these signals over all angles. They set a baseline for calculations of Rayleigh scattering cross-sections from theory, but the reported values in the ultra-violet spectral region deviate from theory and have a high uncertainty ($\pm$11%). CRDS measurements [5,9,14,15] leverage the sensitivity of high finesse cavities to retrieve the scattering cross-section at pressures of 1–100% of ambient pressure by measurements of the change in extinction by the decay of pulsed light in a high-finesse optical cavity. The CRDS measurements agreed very well with refractive index based theoretical calculations (within 1%) over the range investigated (479–650 nm [5,9]) and within 10% in the UV (197–270 nm [14,15]). There have been no measurements of the scattering cross-section by CRDS in the near UV.

With the advent of cavity-enhanced absorption spectroscopy (CEAS) in recent years, the Rayleigh scattering of pure gases has found an application as a calibration standard for high finesse optical cavity instruments. CEAS relies on the absolute scattering cross-sections of gases to calibrate the reflectivity of the mirrors forming the high-finesse cavity. These calibrations in particular use the scattering of helium and nitrogen [17,18]. Recent work by Washenfelder et al. [19] used exponential empirical expressions to represent the scattering cross-section by fitting to the experimental data of Shardanand and Rao [16] and Sneep and Ubachs [5]. With the limited number of data points available in the literature, interpolation of the cross-section between points in the range of 350–480 nm can lead to systematic bias and large uncertainty.

In this work we use cavity ring-down spectroscopy to derive *absolute* Rayleigh scattering cross-section of nitrogen at 532 and 405 nm. We then establish the use of broad-band cavity enhanced spectroscopy for the measurement of *relative* Rayleigh scattering cross-sections of argon, oxygen and air with wavelength coverage from 350 to 700 nm, and calibrate our relative cross-section measurements at a large number of other wavelengths using the CRDS data.

2. Experimental

2.1. Calculations of refractive index based Rayleigh scattering

The scattering cross-sections of the gases investigated (He, N_2, O_2, Ar and air) were calculated with Eq. (1) based on the data for refractive index available in the literature which follow the generalized expression:

$$(n-1)\times 10^8 = A + \frac{B}{C-\nu^2} \tag{2}$$

with terms and their values as described in Table 1, along with the corresponding King correction factor (F_k) equations. The F_k values are taken as unity for mono-atomic gases (He, Ar); for diatomic gases (O_2, N_2) the values are taken from *ab initio* calculations as described in Bates [6], and are estimated to have an uncertainty of <1%. For He, data from references [11–13] are fitted by an expression matching Eq. (2). The Rayleigh scattering cross-section of air was calculated from the expressions given in Bodhaine et al. [7] at 288.15 K and 1013.25 mbar from the refractive index and mixing ratio weighted King correction factors for N_2, O_2, Ar and CO_2.

2.2. Measurements of N_2 Rayleigh scattering by CRDS

The Rayleigh scattering cross-section of N_2 was measured by CRDS using a similar method as that described by Naus and Ubachs [9] and Sneep and Ubachs [5], though the measurements were made at distinct wavelengths of 405.8 nm and 532.2 nm (see Fig. 1). The instrument design has been described previously (Fuchs et al. [20] for 405 nm and references therein; Pettersson et al. [21] for 532 and references therein) and only a brief description of the operation is provided here. A pulse of light is injected into

Table 1
Terms for use in Eq. (2) for the refractive index and for the King correction factor.

Gas	A	B	C	King correction factor	Ref.
He[a,b]	2283	1.8102×10^{13}	1.5342×10^{10}	$F_k(\nu)=1$	[11–13]
N_2[a,c]	5677.465	318.81874×10^{12}	14.4×10^{9}	$F_k(\nu)=1.034+3.17\times10^{-12}\nu$	[5,9]
N_2[a,d]	6498.2	307.4335×10^{13}	14.4×10^{9}	$F_k(\nu)=1.034+3.17\times10^{-12}\nu$	[5,9]
Ar[a,e]	6432.135	286.06021×10^{12}	14.4×10^{9}	$F_k(\nu)=1$	[5,8]
O_2[f,g]	20,564.8	2.480899×10^{13}	4.09×10^{9}	$F_k(\nu)=1.09+1.385\times10^{-11}\nu^2+1.448\times10^{-20}\nu^4$	[5]

[a] Use $N=2.546899\times10^{19}$ molecules cm^{-3} in Eq. (1).
[b] $14{,}285<\nu<33{,}333$ cm^{-1}.
[c] $21{,}360<\nu<39{,}370$ cm^{-1}.
[d] $4860<\nu<21{,}360$ cm^{-1}.
[e] $5000<\nu<33{,}000$ cm^{-1}.
[f] Use $N=2.68678\times10^{19}$ molecules cm^{-3} in Eq. (1).
[g] $18{,}315<\nu<34{,}722$ cm^{-1}.

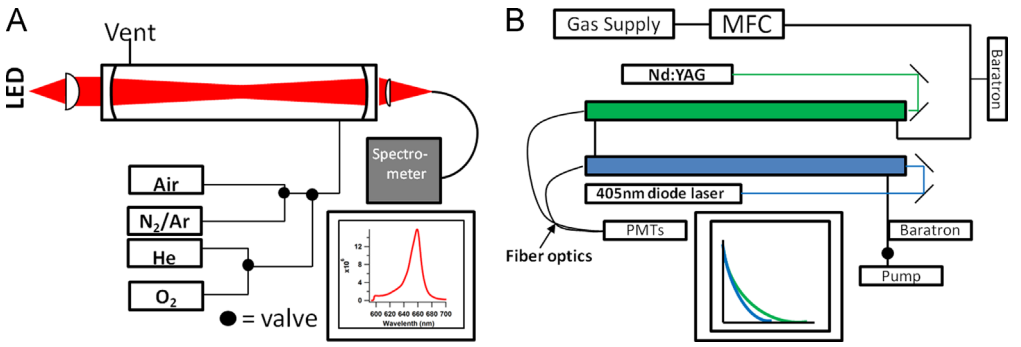

Fig. 1. Sketch of the BBCES set up (A) and CRDS setup (B) used in this study. Also shown are the gas handling, LED light source and spectrometer system for collection of spectra (A). CRDS employed pressure modulation by adjusting the valve downstream of two cavities. Pressure was monitored before and after the cavities to ensure the lack of a pressure gradient.

a cavity capped with highly reflective mirrors (Advanced Thin Films; 405 nm, R=0.99993; 532 nm, R=0.99998), allowing the light to make multiple passes through the cavity. The time, τ, for the signal to decay to $1/e$ of its original intensity was then determined. For a cavity filled only with nitrogen, the only losses are to the mirrors and to Rayleigh scattering by the gas. While the mirror losses will be constant, the loss due to Rayleigh scattering will change with pressure.

Gas was flowed into the cavity at a constant rate using a mass flow controller. A pump was used to remove gas from the cavity, and a valve placed after the cavity but before the pump was used to control the amount of gas removed. Adjusting the valve allowed for control of the pressure inside the cavity. Pressures were adjusted to fixed levels between 80% and 100% of ambient pressure (Boulder, CO; 630 Torr) and were monitored with barometers. The fitted slope of the loss rate ($1/(\tau c)$) in cm^{-1} vs. the density (molecules cm^{-3}) is the Rayleigh scattering cross-section (in cm^2, see Fig. 2). The error is taken from the distribution of retrieved cross-sections between all runs (see Table 2).

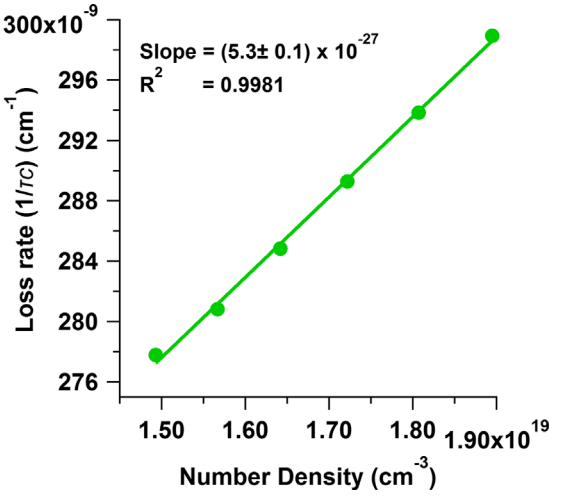

Fig. 2. CRDS measurement of N_2 Rayleigh scattering at 532.2 nm. Each point is the loss-rate at one pressure level. The fitted slope is the scattering cross-section (cm^{-2}).

2.3. Measurements Rayleigh scattering of Ar, O_2 and air by BBCES

The Rayleigh scattering cross-sections of Ar, O_2 and air were measured by Broad-Band Cavity Enhanced Spectroscopy (BBCES). The experimental setup is shown in Fig. 1. First the mirror reflectivity is measured as a function of wavelength with respect to the difference in the extinction due to scattering by He and N_2:

$$R(\lambda) = 1 - d_0 \frac{\left(\frac{I_{N_2}(\lambda)}{I_{He}(\lambda)}\alpha_{Ray}^{N_2}(\lambda)\right) - (\alpha_{Ray}^{He}(\lambda))}{1 - \left(\frac{I_{N_2}(\lambda)}{I_{He}(\lambda)}\right)}. \quad (3)$$

Once the mirror reflectivity has been determined, the Rayleigh scattering can be measured for other gases (O_2, Ar or air) using the following equation (written for the measurement of the O_2 Rayleigh scattering cross-section):

$$\alpha_{Ray}^{O_2} = \left(\left(\frac{1-R(\lambda)}{d_0}\right)\left(1 - \frac{I_{O_2}}{I_{N_2}}\right) + \alpha_{Ray}^{N_2}\right)\left(\frac{I_{N_2}}{I_{O_2}}\right) \quad (4)$$

where $\alpha_{Ray}^{O_2}$ is the extinction per length (cm^{-1}) due to Rayleigh scattering by O_2 (or N_2), $R(\lambda)$ is the mirror reflectivity with respect to wavelength, I is the intensity in each gas, and d_0 is the cavity length. Dividing this quantity ($\alpha_{Ray}^{O_2}$, the extinction) by the density of the gas yields the Rayleigh scattering cross-section. For the calculation of the mirror curve the Rayleigh scattering cross-section for He is taken from the fitted expression of Washenfelder et al. [19] as the relatively high uncertainty is masked by the cross-section being 2 orders of magnitude smaller than N_2 (the intensity of light incident on the detector for the various gases is shown in Fig. S1 in the Supplementary Material). The use of the refractive index based (hereafter referred to as n-based) theory values of He instead of the fitted expression leads to a $<0.1\%$ change in the mirror transmission (reflectivity) curve. The N_2 cross-section used is calculated from the theory given in Table 1. This measurement is done relative to the known value of the N_2 Rayleigh scattering cross-section and the mirror curve (R, measured based on the scattering of He and N_2, Eq. (3)). It is not an independent measurement of the absolute Rayleigh scattering cross-section as it is measured with CRDS. The advantage of this approach is the ability to measure at many wavelengths simultaneously over a wide wavelength range. This multiplexing advantage of BBCES (600–1000 individual wavelengths are measured simultaneously, see Fig. 3) adds wavelength resolved information,

Table 2
Rayleigh scattering cross-sections ($cm^{-3} \times 10^{27}$) from RI based theory and experiments for selected wavelengths.

	N_2		Ar		O_2		Air	
λ (nm)	Theory	Exp[a,c]	Theory	Exp[b,c]	Theory	Exp[b,c]	Theory	Exp[b,c]
370.0	23.698	–	20.361	20.2(3)	21.269	21.4(3)	23.183	23.0(3)
405.8	16.146	16.1(1)	13.881	14.0(2)	14.373	14.4(2)	15.765	15.7(2)
532.2	5.302	5.32(2)	4.563	4.57(6)	4.740	–	5.159	–
660.0	2.988	–	1.904	1.91(2)	1.935	1.96(3)	2.148	2.15(3)

[a] CRDS data.
[b] BBCES data.
[c] Number in () is the $1-\sigma$ error in the reported value of the last digit for BBCES and the range for CRDS.

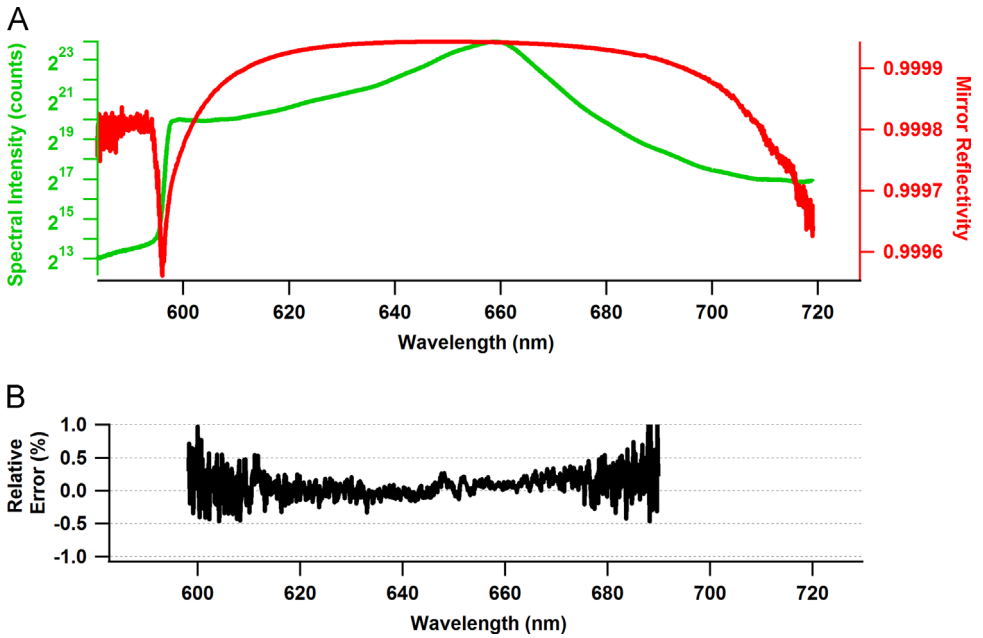

Fig. 3. BBCES uncertainty in Ar Rayleigh scattering cross-sections with respect to signal intensity and mirror reflectivity. (A) Example for spectral data near 660 nm; (B) the relative error compared to *n*-based theory is calculated as [absolute value(Measurement – theory)/Theory × 100] as a function of wavelength.

and greatly increases the number of available measurements for the benefit of reducing error (see Section 2.4).

Measurements were performed using cavities with center wavelengths and reflectivities of 365 nm (0.99985), 405 nm (0.99995), 455 nm (0.999972), 532 nm (0.99998), 580 nm (0.999978) and 630 nm (0.99993) (Advanced Thin Films – 365, 405, 455 and 532 nm; CRD-optics – 580 nm; and Los Gatos – 630 nm, see Thalman and Volkamer [22]). O_2 and air scattering were retrieved at wavelengths in between the O_4 absorption bands (see Fig. 4). Spectra were recorded with an Acton 2300i spectrometer using a PIXIS 400b CCD detector (see Coburn et al. [23] for details of the spectrometer/detector system).

2.4. Error propagation for BBCES

The measurement uncertainty for BBCES can be assessed by the propagation of the errors associated with the measurements. The pressure ($\pm 0.1\%$), temperature ($\pm 0.3\%$) and cavity length (87 ± 0.1 cm) are combined with the Rayleigh cross-section uncertainties for N_2 ($\pm 1\%$) and He ($\pm 5\%$) as well as the photon counting uncertainty in the spectra ($\ll 1\%$) to get an overall relative uncertainty for the mirror reflectivity curve of $\pm 1.1\%$. Carrying the propagation through to the measurement of the Rayleigh cross-section leads to a measurement uncertainty of $\pm 1.3\%$ at the center of the mirror and $\pm 2\%$ at the far extremes of the mirror range.

In Fig. 3, 783 individual measurements show a deviation $< 1.3\%$ (the absolute error of a single BBCES measurement). The relative deviation from *n*-based theory near 660 nm in our BBCES measurements is on average $0.055 \pm 0.005\%$, which corresponds to an agreement with *n*-based theory of better 0.66% at the 95% confidence interval (see Fig. 5 for statistical analysis).

3. Results

3.1. Nitrogen

The results of the CRDS measurements of the N_2 Rayleigh scattering cross-section are shown in Table 2 with values calculated from theory and the percent

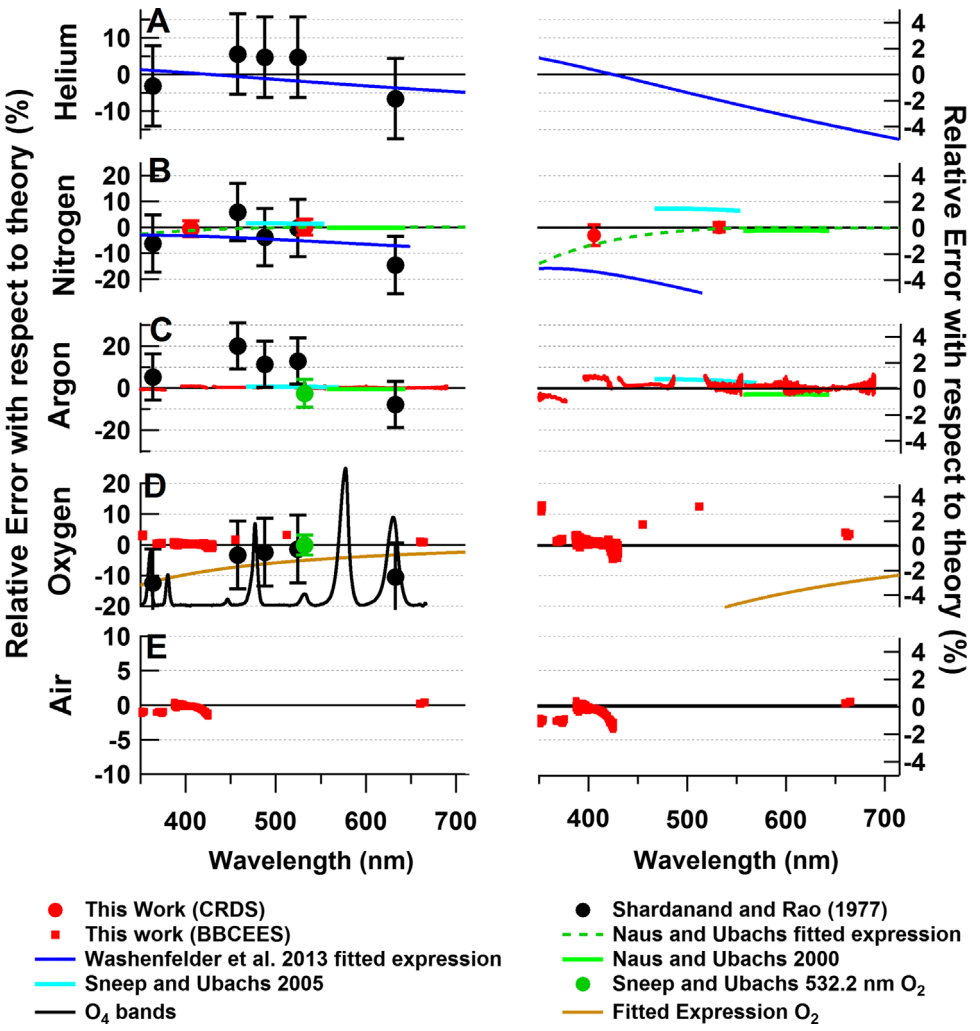

Fig. 4. Deviations of measured Rayleigh scattering cross-sections from refractive index based theory for this work (red dots/circles) and previous work (see legend). The left panels show the full range of values while the right panels show each gas with a range of ±5% deviation from theory and omits individual literature data points for clarity. Panel (A) shows the deviation of the literature values for He. The remaining panels show the deviations of the literature values and measurements from this work with respect to the theory for N_2 (B), Ar (C), O_2 (D), air (E). The O_4 bands are shown in panel D for reference. (For interpretation of the references to color in this figure legend, the reader is referred to the web version of this article.)

deviation relative to theory ([(experiment − theory)/theory] × 100) is shown in Fig. 4 panel B along with the relevant literature data. The agreement of the measurement at 405 nm is within 1% of the theory. A limited number of sets of data were able to be taken so the error in Table 2 is expressed as the range of repeat measurements. Shown in the figure are the available literature data [5,9,16] as well as the deviation of the exponential fits of Naus and Ubachs [9]. This fit is representative over the range it was fit (500–700 nm) but begins to diverge from the theory at shorter wavelengths. The fit by Washenfelder et al. [19] deviates by up to 10% from the refractive index based calculation and our CRDS measurement.

3.2. Argon

The results of the BBCES measurements of the Ar Rayleigh scattering cross-section are shown along with the literature data relative to the *n*-based theory from 350 to 700 nm in Fig. 4 panel C. The BBCES measurements agree within better than 1% with the calculated numbers for the entire wavelength range. The variability near the edges of the mirrors (and light sources) can be observed for each set of mirrors in Fig. 3. We limit the range of values shown here to the spectral ranges where the agreement is better than 1%. For more detail see Fig. S2 in the Supplementary material. Further binning of the results relative to *n*-based theory for each cavity individually shows that the UV, near-UV and blue data show small systematic bias compared to *n*-based theory (−0.64, 0.865%, and 0.3%, respectively), while for the red, amber and green wavelength cavities the mean of the distribution are within 0.2% (95% confidence interval) indistinguishable from theory (see Fig. 5).

3.3. Oxygen

Measurements of the O_2 Rayleigh scattering cross-section are displayed along with the literature data relative

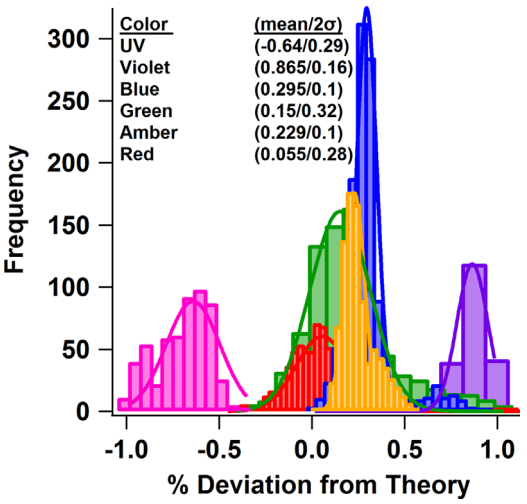

Fig. 5. Histograms of the deviation of measurements of Ar σ_{Ray} broken out by cavity. The mean and $2-\sigma$ standard deviation of the distribution are shown in the inset. The dataset averaged mean (of all cavities) is $0.2 \pm 0.4\%$.

to the cross-section calculated from theory in Fig. 4 panel D. Data is only used between the O_4 absorption bands from 370 to 660 nm [22,24]. The *n*-based theory is consistent within 1% for ranges with no O_4 bands (370–420 nm and 660 nm) and $<4\%$ for the portions of the spectrum that are located between adjacent O_4 bands (340, 440, 460 and 520 nm).

3.4. Air

Measurements of the Rayleigh scattering cross-section of air are displayed in Fig. 4 panel E relative to the theory calculations as given by Penndorf [25] and Bodhaine et al. [7]. Reported data is from the windows in between the O_4 absorption bands and agrees within 1% of theory.

3.5. Literature comparison for He theory and measurements

The one available set of literature values [16] for He are compared to the theory in Fig. 4 panel A. Also shown are the empirical exponential fit to the literature data [19] and the deviation from the theory of both the data as well as the fit to the data. The fit to the available data does a reasonable ($<5\%$ variation) job of representing the theory; the measured data scatters around the theory line. Based on the comprehensive evidence from this work that theory represents measurements for other gases very well (within 1%), the larger relative error of Helium measurements, and the fact that King correction factors are unity, we conclude that theory represents the most accurate Rayleigh scattering cross section values also for Helium.

4. Discussion and conclusion

The measurements of the N_2 Rayleigh scattering cross-section by cavity-ring down spectroscopy (CRDS) agree with *n*-based theory within error bounds, and extend the validation of the theory into the near-UV spectral range. The uncertainty of the cavity measurements from the propagation of errors in pressure, temperature and the length of the cavity as well as the N_2 and He (for mirror reflectivity calibration) cross-sections is $\pm 1.3\%$. Using the absolute measurements made with CRDS, we have further demonstrated measurements of Rayleigh scattering cross-sections by Broad-Band Cavity Enhanced Spectroscopy (BBCES). We have measured Ar, O_2 and air cross sections with BBCES relative to those of N_2, and find agreement within 0.1–0.9% with *n*-based theory calculations (see Fig. 5 and Table 2). The best agreement is typically found near the center peak of reflectivity curves of mirrors with BBCES, with slightly larger differences near the edges of the reflectivity curves. We note that lower mirror reflectivity (and thus lower sensitivity) and lower signal intensity (higher photon shot noise) lead to similar trends in the relative error in the Rayleigh scattering cross sections derived in this work (Fig. S2), and cannot be distinguished in these experiments (see Supplementary material).

The Rayleigh scattering cross-sections underlie the determination of the reflectivity of mirror curves with CEAS techniques that determine the absorption path length. A 1% bias in the Rayleigh scattering cross-section (mostly N_2) translates to a 1% bias in the mirror reflectivity. This error further propagates to the characterization of trace gas concentrations, absorption cross-section spectra, or light absorption/extinction by aerosols. The extinction due to Rayleigh scattering can become comparable to the loss due to the mirror for highly reflective mirrors ($R > 0.9999$; depending on the wavelength of light). Thus, use of an incorrect Rayleigh cross-section can have a relatively larger bias in the data analysis step (calculation of the extinction (α) see Eq. (4)) compared to lower reflectivity mirrors (i.e. UV mirrors, $R=0.9998$). For example, for two sets of mirrors at 455 nm with reflectivities of 0.9998 and 0.99997 and a 5% low bias in the nitrogen cross-section used to calibrate the mirror reflectivity, the resulting biases are 4.8% and 2.8% respectively when this biased reflectivity curve is used to interpret spectra taken in air. Using a biased σ_{Ray} of air in the calculation of extinction would further increase the overall bias. The effect of any bias in σ_{Ray} of N_2 for mirror reflectivity calculations is partly muted with using higher reflectivity mirrors when the extinction due to Rayleigh scattering becomes similar to the extinction of mirror losses (see Figs. S3 and S4 in the Supplementary Material). We have investigated the effect of different O_2 Rayleigh scattering cross sections on our earlier reports about O_4 absorption cross-section spectra [22]. Use of the fitted expression for O_2 Rayleigh scattering cross-sections [19] differs by $>10\%$ from the *n*-based theory (Fig. S4), and can lead to bias in the retrieved O_4 cross-section of $<2.5\%$ at 360 nm, and -2.8% at 446 nm. However, even differences $<1\%$ are discernible outside error bars in the comparison of DOAS retrievals of O_4 slant column densities and O_4 predictions [17,22]. We find that the measured O_4 slant column density agrees within $-0.3 \pm 0.5\%$ with that predicted. This excellent agreement from measuring a calibration trace gas is only observed using Rayleigh cross sections calculated from *n*-based theory to derive mirror curves that are confirmed with little error in this study.

We conclude:

(1) The combination of BBCES and CRDS provides wavelength resolved and accurate measurements of Rayleigh scattering cross sections. BBCES efficiently provides information at many wavelengths from a single measurement, at a single gas density, relative to a reference gas (here N_2).
(2) Our data present experimental confirmation for Rayleigh scattering cross-sections calculated from *n*-based theory within $0.2 \pm 0.4\%$ at all investigated wavelengths. Our multispectral measurements extend the spectral range over which *n*-based theory has been compared to observations of the Rayleigh scattering of Ar, air and O_2. In particular, we provide data in the near-UV range with low uncertainty, where only one set of measurements had previously been available.
(3) Rayleigh scattering cross sections based on *n*-based theory are better suited than empirical fit expressions to calibrate techniques based on cavity enhanced absorption/extinction spectroscopy (CEAS/BBCES). The relative retrieval of Ar Rayleigh scattering cross sections serves as a useful verification of mirror reflectivity calculations.

Previous measurements for Rayleigh scattering cross-sections of He compare favorably to theory, but are not represented well by exponential fits to the available experimental data. While the uncertainty in the He Rayleigh scattering cross-section contributes only a small portion to the error of CEAS measurements, we recommend the use of *n*-based theory also for He to calibrate CEAS/BBCES instruments. Further measurements of the Rayleigh scattering cross-section of He by CRDS at wavelengths from 355 to 532 would be a valuable addition to the available literature.

Acknowledgments

RMT is the recipient of a CIRES Graduate Research Fellowship. This work was supported by the National Science Foundation CAREER award ATM-847793 and CU start-up funds for RV. MAT and KJZ gratefully acknowledge National Aeronautics and Space Administration Grant NNX09AE12G.

Appendix A. Supporting information

Supplementary data associated with this article can be found in the online version at http://dx.doi.org/10.1016/j.jqsrt.2014.05.030.

References

[1] Strutt JW. (Lord Rayleigh). On the transmission of light through an atmosphere containing small particles in suspension, and on the origin of the blue of the sky. Philos Mag 1899;47:375–84.
[2] Strutt JW. (Lord Rayleigh). A re-examination of the light scattered by gases in respect of polarisation. I. Experiments on the common gases. Proc R Soc Lond Ser A 1920;97(687):435–50.
[3] King LV. On the complex anisotropic molecule in relation to the dispersion and scattering of light. Proc R Soc Lond Ser A 1923;104(726):333–57.
[4] Strutt RJ. The light scattered by gases: its polarisation and intensity. Proc R Soc Lond. Ser A 1918;95(667):155–76.
[5] Sneep M, Ubachs W. Direct measurement of the Rayleigh scattering cross section in various gases. J Quant Spectrosc Radiat Transfer 2005;92(3):293–310.
[6] Bates DR. Rayleigh-Scattering by Air. Planet Space Sci 1984;32(6):785–90.
[7] Bodhaine BA, Wood NB, Dutton EG, Slusser JR. On Rayleigh optical depth calculations. J Atmos Ocean Technol 1999;16(11):1854–61.
[8] Eberhard WL. Correct equations and common approximations for calculating Rayleigh scatter in pure gases and mixtures and evaluation of differences. Appl Opt 2010;49(7):1116–30.
[9] Naus H, Ubachs W. Experimental verification of Rayleigh scattering cross sections. Opt Lett 2000;25(5):347–9.
[10] Abjean R, Mehu A, Johannin A. Interferometric measurement of refraction indices of nitrogen and argon in ultraviolet. C R Hebd Seances Acad Sci Ser B 1970;271(7):411–4.
[11] Abjean R, Mehu A, Johannin A. Interferometric measurement of refraction indices of helium and neon in ultra violet. C R Hebd Seances Acad Sci Ser B 1970;271(16):835.
[12] Leonard PJ. Refractive indices, Verdet constants, and polarizabilities of the inert gases. At Data Nucl Data Tables 1974;14(1):21–37.
[13] Cuthbertson C, Cuthbertson M. The refraction and dispersion of neon and helium. Proc R Soc Lond Ser A Contain Pap Math Phys Character 1932;135(826):40–7.
[14] Ityaksov D, Linnartz H, Ubachs W. Deep-UV Rayleigh scattering of N_2, CH_4 and SF_6. Mol Phys 2008;106(21–23):2471–9.
[15] Ityaksov D, Linnartz H, Ubachs W. Deep-UV absorption and Rayleigh scattering of carbon dioxide. Chem Phys Lett 2008;462(1–3):31–4.
[16] Shardanand Rao ADP. Absolute Rayleigh scattering cross sections of gases and freons of stratospheric interest in the visible and ultraviolet regions. NASA Technical Note TN-D-8442; 1977.
[17] Thalman R, Volkamer R. Inherent calibration of a blue LED-CE-DOAS instrument to measure iodine oxide, glyoxal, methyl glyoxal, nitrogen dioxide, water vapour and aerosol extinction in open cavity mode. Atmos Meas Tech 2010;3(6):1797–814.
[18] Washenfelder RA, Langford AO, Fuchs H, Brown SS. Measurement of glyoxal using an incoherent broadband cavity enhanced absorption spectrometer. Atmos Chem Phys 2008;8(24):7779–93.
[19] Washenfelder RA, Flores JM, Brock CA, Brown SS, Rudich Y. Broadband measurements of aerosol extinction in the ultraviolet spectral region. Atmos Meas Tech 2013;6(4):861–77.
[20] Fuchs H, Dubé WP, Lerner BM, Wagner NL, Williams EJ, Brown SS. A sensitive and versatile detector for atmospheric NO_2 and NO_X based on blue diode laser cavity ring-down spectroscopy. Environ Sci Technol 2009;43(20):7831–6.
[21] Pettersson A, Lovejoy ER, Brock CA, Brown SS, Ravishankara AR. Measurement of aerosol optical extinction at 532 nm with pulsed cavity ring down spectroscopy. J Aerosol Sci 2004;35(8):995–1011.
[22] Thalman R, Volkamer R. Temperature dependent absorption cross-sections of O_2–O_2 collision pairs between 340 and 630 nm and at atmospherically relevant pressure. Phys Chem Chem Phys 2013;15(37):15371–81.
[23] Coburn S, Dix B, Sinreich R, Volkamer R. Atmos Meas Tech 2011;4:2421–39.
[24] Hermans C, Vandaele A, Carleer M, Fally S, Colin R, Jenouvrier A, et al. Absorption cross-sections of atmospheric constituents: NO_2, O_2, and H_2O. Environ Sci Pollut Res 1999;6(3):151–8.
[25] Penndorf R. Tables of the refractive index for standard air and the Rayleigh scattering coefficient for the spectral region between 0.2 and 20.0-mu and their application to atmospheric optics. J Opt Soc Am 1957;47(2):176–82.